12th IFAC International Symposium on
Advanced Control of Chemical Processes
July 14-17, 2024. Toronto, Canada

Distributed Estimation and Control of Process Networks using Adaptive Community Detection

Amirmohammad Ebrahimi and **Davood B. Pourkargar** ⋆

Tim Taylor Department of Chemical Engineering
Kansas State University, Manhattan, KS 66506 USA

Abstract: An integrated distributed moving horizon estimation (DMHE) and model predictive control (DMPC) approach is developed for complex process networks using an adaptive spectral community detection-based decomposition. The proposed approach employs the weighted graph representation of the process network model to identify optimal communities for distributed estimation and control architectures. The resulting decomposition dynamically adapts as the network transitions across different operating conditions. Consequently, adjustments are made to the integrated DMHE and DMPC architecture to optimize closed-loop performance and enhance robustness. A benchmark benzene alkylation process under various operating conditions is employed to substantiate the proposed methodology's efficacy. Simulation results demonstrate the effectiveness of the proposed method, showing improved closed-loop performance and computational efficiency compared to traditional unweighted hierarchical community detection-based decompositions.

Keywords: Nonlinear process control, model predictive and optimization-based control, distributed control and estimation, graph-based methods for networked systems, process control

1. INTRODUCTION

The widespread adoption of integrated processes, driven by the imperative to reduce costs, optimize resource consumption, and enhance process efficiency, particularly in reducing material waste and energy use, poses significant operational and control challenges. The intricate dynamics of these integrated processes are exacerbated by the nonlinear behavior of individual units and the interactions arising from their connectivity and recycle streams, intensifying overall process nonlinearity and complexity (Baldea and Daoutidis [2012]). Model Predictive Control (MPC), a sophisticated technique offering substantial advantages over alternative methods (Schwenzer et al. [2021]), addresses these challenges by transforming the control problem into an optimization task. However, the real-time solution of dynamic optimization problems, subject to process constraints for determining manipulated inputs, as MPC requires, imposes considerable computational burdens (Lopez-Negrete et al. [2013], Rawlings et al. [2017]). These burdens result in significant time delays, particularly in highly integrated processes (Lopez-Negrete et al. [2013], Pannocchia et al. [2007], Wang and Boyd [2009]), leading to undesirable products and financial losses due to delays in controller decision-making.

Distributed model predictive control (DMPC) is an efficient alternative to centralized MPC, offering faster computations while maintaining control quality comparable to the centralized approach. In DMPC, multiple control agents collaborate to address the dynamic optimization problem, diverging from the reliance on a single agent in centralized MPC. The initial step in implementing DMPC involves decomposing the control structure, determining the number of communities, and allocating manipulated inputs, controlled outputs, and constraints among them. An optimal decomposition minimizes community interaction, implying that when dividing the control system into P subsystems, each subsystem ideally makes autonomous decisions with minimal interference from others (Leicht and Newman [2008]).

The exploration of optimal decomposition, referred to as community detection, has been the subject of extensive research, with a primary focus on hierarchical approaches based on network adjacency matrix (Heo and Daoutidis [2016], Heo et al. [2015], Leicht and Newman [2008], Tang et al. [2018a]). Community detection involves identifying subsystems that exhibit heightened internal density within the subsystem or diminished connectivity across distinct subsystems (Newman [2006]). The effectiveness of community detection algorithms is quantitatively evaluated using modularity, which measures the proportion of edges (or weights) covered by communities compared to their expected value in a randomized graph. Optimizing modularity involves minimizing linkages between subsystems or maximizing connections within individual subsystems (Leicht and Newman [2008]). Utilizing an input-output bipartite graph as the basis for community detection has been explored by Tang and Daoutidis [2018], along with

⋆ Corresponding Author, Email: dbpourkargar@ksu.edu, Tel: +1 (785) 532-5584, Fax: +1 (785) 532-7372.
This research is based upon work supported by the National Science Foundation under grant no. OIA-2148878 and the State of Kansas through the Kansas Board of Regents.

Copyright © 2024 the authors. Accepted by IFAC for publication under a Creative Commons License CC-BY-NC-ND.

using long-time and short-time responses for detecting optimal communities (Tang et al. [2018b]). Community detection based on unweighted graphs has been studied by Newman [2013] and later extended to weighted networks (Jogwar [2019]). The spectral properties of unweighted graphs for community detection were initially investigated by Newman [2013]. This approach was subsequently extended to weighted networks by Jogwar [2019].

Solving MPC problems requires real-time access to state values. While previous studies have made this assumption, practical scenarios often limit the feasibility of measuring all states using sensors. Moving Horizon Estimation (MHE) has emerged as a compelling alternative for estimating unmeasurable values based on historical data, as it can be formulated as a dynamic optimization problem similar to MPC (Rao et al. [2003], Rawlings and Bakshi [2006]). However, like MPC, solving such optimization problems for large-scale, highly integrated systems is computationally expensive. Delays in estimation can compromise closed-loop control system performance, given that control decisions rely on knowledge of all states (Guay et al. [2015]). In response to the computational challenges of centralized estimation, a strategy akin to the DMPC method, namely the DMHE framework, is employed. This framework comprises local estimators that collaboratively share information (Pourkargar et al. [2019], Yin et al. [2018], Yin and Liu [2019]). A unified min-max optimization approach is proposed, combining centralized MPC and MHE (Copp and Hespanha [2014, 2017]), demonstrating that the estimated states remain bounded under the assumptions of controllability and observability of nonlinear processes. Unlike centralized implementations, distributed designs using community detection-based decompositions enable expedited computations without significant performance degradation. Case studies on a benchmark reactor-separator process network, the benzene alkylation process with ethylene, and an amine gas sweetening plant, conducted on different optimization platforms, with varying communication patterns between local controllers and accounting for model uncertainty, reveal the efficacy of this approach (Pourkargar et al. [2017a,b, 2019]). Prior research has predominantly focused on hierarchical community detection for optimal decompositions in control and estimation based on an unweighted network.

The primary objective of this study is to understand how interactions among network components influence the optimal decomposition of control and estimation problems across diverse operational settings. Specifically, this work explores the creation of distributed control and estimation architectures and assesses the computational efficiency of the corresponding decomposition processes. In contrast to conventional hierarchical community detection methods that iteratively divide subsystems until achieving relatively high modularity, our proposed methodology employs spectral community detection. This approach efficiently divides the system into the intended number of subsystems in a single iteration, leveraging graph spectral properties to assess component closeness and assign them to specific subsystems. The resulting integrated DMHE and DMPC based on adaptive spectral community detection-based decomposition are applied to regulate a benchmark benzene alkylation process. Evaluation of closed-loop performance and computation time is conducted under varying operating conditions. Simulation results underscore the efficacy of the adaptive community detection-based distributed control and estimation method in regulating critical characteristics of the benzene alkylation process. Moreover, the study highlights differences in optimal decomposition across different operational circumstances. The subsequent sections of the paper are organized as follows: Section 2 presents the nonlinear process network model, its characteristics, and the mathematical formulation of nonlinear MPC, MHE, DMPC, and DMHE. Section 3 provides detailed insights into forming control and estimation networks, developing an adaptive community detection approach rooted in weighted graphs, and the design of a distributed architecture. Finally, Section 4 presents the results of the benzene alkylation simulation study.

2. PROBLEM DESCRIPTION

2.1 Process model

Consider the following general nonlinear state-space model, which describes the process network dynamics

$$\begin{aligned} &\dot{x}(t) = f(x(t), u(t)) + \omega(t), \quad y(t) = g(x(t), u(t)) \\ &\hat{y}(t) = h(x(t), u(t)) + \nu(t) \end{aligned} \tag{1}$$

where $x(t) \in \mathbb{R}^n$ represents the vector of state variables, $u(t) \in \mathbb{R}^m$ is the vector of manipulated inputs, $\omega(t) \in \mathbb{R}^n$ denotes the vector of additive disturbances to the process, $y(t) \in \mathbb{R}^r$ is the vector of controlled outputs, $\hat{y}(t) \in \mathbb{R}^s$ represent the vector of measured outputs, $\nu(t) \in \mathbb{R}^s$ is the vector of measurement noises, t is the time, and $f : \mathbb{R}^n \times \mathbb{R}^m \to \mathbb{R}^n$, $g : \mathbb{R}^n \times \mathbb{R}^m \to \mathbb{R}^r$, and $h : \mathbb{R}^n \times \mathbb{R}^m \to \mathbb{R}^s$ are smooth nonlinear functions. The equilibrium point for the process network model in its unforced state is assumed to be at the origin.

2.2 Integrated MPC and MHE formulation

The centralized MPC problem for the process network model of 1 can be formulated as follows

$$\begin{aligned} \min_u \int_{t_k}^{t_k+N_cT} &\big((y - y^{\text{ss}})^T P (y - y^{\text{ss}}) \\ &+ (u - u^{\text{ss}})^T W (u - u^{\text{ss}})\big) dt \end{aligned} \tag{2}$$

subject to the system constraints

$$\begin{aligned} &\dot{x} = f(x, u) + \omega, \quad y = g(x, u), \quad u^{\min} \le u \le u^{\max} \\ &\xi(x, u, t) \le 0, \quad \phi(x, u, t) = 0 \end{aligned} \tag{3}$$

The notations t_k, N_c, and T represent the k-th sampling time, the number of sampling times in the control horizon, and the sampling period, respectively. The vectors $y^{\text{ss}}(t) \in \mathbb{R}^r$ and $u^{\text{ss}}(t) \in \mathbb{R}^m$ represent the desired controlled outputs and corresponding steady-state manipulated inputs, respectively. Furthermore, the optimization problem's objective function incorporates two positive definite matrices denoted as $P \in \mathbb{R}^{r \times r}$ and $W \in \mathbb{R}^{m \times m}$ to penalize the output regulation errors and the magnitude of the inputs in the MPC's underlying dynamic optimization problem. The lower and upper bounds of the manipulated input vector are denoted by $u^{\min} \in \mathbb{R}^m$ and $u^{\max} \in \mathbb{R}^m$, respectively. This study also considers generic nonlinear vector functions of ξ and ϕ to describe inequality and equality constraints. The vector of manipulated variables is determined by solving the dynamic optimization problem described by Eqs. 2 and 3 within the control horizon

$[t_k, t_k + N_c T]$. At time t_k, only the first element of the calculated manipulated inputs trajectory is applied to the process in the subsequent time step, $t \in [t_k, t_k + T]$. The prediction horizon then advances by a time step, prompting the optimization problem to be reformulated with a new prediction horizon, $[t_k + T, t_k + (N_c + 1)T]$.

The centralized MHE for estimating the unmeasured state variables can also be formulated as follows

$$\min_{x_k} \int_{t_k - N_m T}^{t_k} \left(\nu^T R \nu + \omega^T Q \omega\right) dt \tag{4}$$

subject to the system constraints

$$\begin{aligned} &\dot{x} = f(x,u) + \omega, \;\; \hat{y} = g(x,u) + \nu \\ &x_k^{\min} \le x_k \le x_k^{\max}, \quad \xi(x,u,t) \le 0, \quad \phi(x,u,t) = 0 \end{aligned} \tag{5}$$

The variable x_k denotes the vector of immeasurable states necessitating estimation. The variable N_m represents the number of sample instances employed in the MHE. Additionally, $R \in \mathbb{R}^{s \times s}$ and $Q \in \mathbb{R}^{n \times n}$ denote positive definite weight matrices utilized to penalize disturbances and noise, respectively. The upper and lower bounds for x_k are represented by $x_k^{min} \in \mathbb{R}^s$ and $x_k^{max} \in \mathbb{R}^s$, respectively. Fig. 1 illustrates the integration of MHE and MPC.

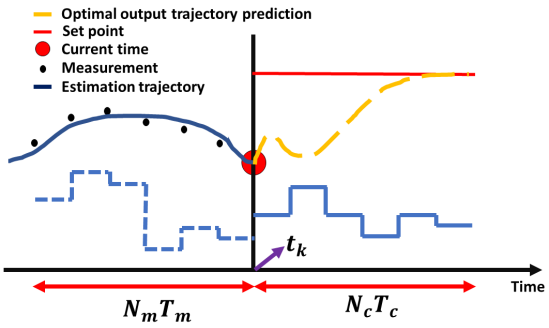

Fig. 1. A schematic of integrated MHE and MPC.

2.3 Distributed architecture and DMPC/DMHE design

Consider the control problem discussed previously for the system described by the state space model 1. Assume that the process network can be decomposed into L subsystems, each of which can be represented by the following submodels

$$\begin{aligned} &\dot{x}_{(i)}(t) = f_{(i)}(x(t), u_{(i)}(t)) + \omega_{(i)}(t), \quad i = 1, \ldots, L \\ &y_{(i)}(t) = g_{(i)}(x(t), u_{(i)}(t)) \end{aligned} \tag{6}$$

where $x = [x_{(1)}^T \; x_{(2)}^T \ldots x_{(L)}^T]^T$, $u = [u_{(1)}^T \; u_{(2)}^T \ldots u_{(L)}^T]^T$, $\omega = [\omega_{(1)}^T \; \omega_{(2)}^T \ldots \omega_{(L)}^T]^T$, $y = [y_{(1)}^T \; y_{(2)}^T \ldots y_{(L)}^T]^T$, $f = [f_{(1)}^T \; f_{(2)}^T \ldots f_{(L)}^T]^T$, and $g = [g_{(1)}^T \; g_{(2)}^T \ldots g_{(L)}^T]^T$ with $f_{(i)} : \mathbb{R}^n \times \mathbb{R}^{m_i} \to \mathbb{R}^{n_i}$ and $g_{(i)} : \mathbb{R}^n \times \mathbb{R}^{m_i} \to \mathbb{R}^{r_i}$ denote the respective components of functions f and g for the i-th subsystem. The state variables, manipulated inputs, additive disturbance, and output variables of i-th subsystem are described by $x_{(i)} = [x_{(i),1}^T \; x_{(i),2}^T \ldots x_{(i),n_i}^T]^T$, $u_{(i)} = [u_{(i),1}^T \; u_{(i),2}^T \ldots u_{(i),m_i}^T]^T$, $\omega_{(i)} = [\omega_{(i),1}^T \; \omega_{(i),2}^T \ldots \omega_{(i),n_i}^T]^T$, and $y_{(i)} = [y_{(i),1}^T \; y_{(i),2}^T \ldots y_{(i),r_i}^T]^T$, respectively, where $n = \sum_{i=1}^L n_i$, $m = \sum_{i=1}^L m_i$ and $r = \sum_{i=1}^L r_i$.

The DMPC problem for the i-th control agent assigned to the i-th subsystem is formulated as follows

$$\begin{aligned} \min_{u_{(i)}} \int_{t_k}^{t_k + N_c T} &\big((y_{(i)} - y_{(i)}^{\text{ss}})^T P_{(i)} (y_{(i)} - y_{(i)}^{\text{ss}}) \\ &+ (u_{(i)} - u_{(i)}^{\text{ss}})^T W_{(i)} (u_{(i)} - u_{(i)}^{\text{ss}})\big) dt \end{aligned} \tag{7}$$

subject to

$$\begin{aligned} &\dot{x} = f(x,u) + \omega, \;\; y_{(i)} = g_{(i)}(x,u) \\ &u_{(i)}^{\min} \le u_{(i)} \le u_{(i)}^{\max}, \quad \xi(x,u,t) \le 0, \quad \phi(x,u,t) = 0 \end{aligned} \tag{8}$$

where the positive definite matrices $P_{(i)}$ and $W_{(i)}$ penalize the output regulation errors and the magnitude of the inputs associated with the i-th control agent. At each sampling time, the control agents compute the sequences for optimal manipulated input vectors for the associated subsystems by solving the optimization problems outlined in 7 and 8. Following this computation, the control agents exchange these manipulated input sequences. Subsequently, each control agent reevaluates the manipulated input vector. This iterative process continues until the discrepancy in magnitude between two successively manipulated input vectors falls below a predefined threshold.

Similar to the control network decomposition, the estimation problem for the system described by Eq. 1 can be partitioned into N subsystems, as detailed below

$$\begin{aligned} &\dot{x}_{(j)}(t) = f_{(j)}(x(t), u(t), t) + \omega_{(j)}(t), \quad j = 1, \ldots, N \\ &\hat{y}_{(j)}(t) = h_{(j)}(x(t), u(t)) + \nu_{(j)}(t) \end{aligned} \tag{9}$$

where $\hat{y} = [\hat{y}_{(1)}^T \; \hat{y}_{(2)}^T \ldots \hat{y}_{(N)}^T]^T$ and $h = [h_{(1)}^T \; h_{(2)}^T \ldots h_{(N)}^T]^T$. The measurement noises for j-th subsystem is represented by $\nu_{(j)} = [\nu_{(j),1}^T \; \nu_{(j),2}^T \; \ldots \; \nu_{(j),s_j}^T]^T$ with $s = \sum_{j=1}^N s_j$.

The DMHE problem for the j-th estimator agent can be formulated as follows

$$\min_{x_{k,(j)}} \int_{t_k - N_m T}^{t_k} \left(\nu_{(j)}^T R_{(j)} \nu_{(j)} + \omega_{(j)}^T Q_{(j)} \omega_{(j)}\right) dt \tag{10}$$

subject to

$$\begin{aligned} &\dot{x} = f(x,u,t) + \omega, \;\; \hat{y}_{(j)} = g_{(j)}(x,u,t) + \nu_{(j)} \\ &x_{k,(j)}^{\min} \le x_{k,(j)} \le x_{k,(j)}^{\max} \\ &\xi(x,u,t) \le 0, \quad \phi(x,u,t) = 0 \end{aligned} \tag{11}$$

The positive definite matrices $R_{(j)}$ and $Q_{(j)}$ are introduced to penalize the measured outputs and estimated state variables of the j-th subsystem, respectively. Like DMPC, the j-th local estimator estimates the immeasurable state values of the j-th subsystem at each sampling instance and shares these values with other estimators. Subsequently, each local estimator updates its estimated values based on the information received from other estimators. This iterative process continues until the magnitude difference between the vectors of estimated states from two consecutive iterations falls below a predetermined threshold. Figure 2 presents a block diagram of integrated DMHE and DMPC.

3. ADAPTIVE DISTRIBUTED ARCHITECTURE DESIGN

This section investigates the optimal system decomposition for integrated process networks, aiming to design a distributed estimation and control architecture adaptable to varying operational conditions. The proposed approach leverages the weighted graph representation of the process systems, generating an adjacency matrix that describes

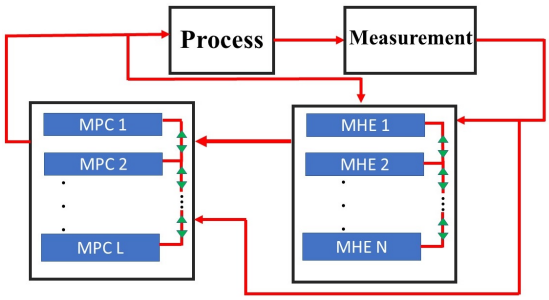

Fig. 2. Integrated DMHE and DMPC block diagram (L local control agents and N local estimation agent).

dynamic relationships among input, state, and output variables. Modularity metrics are then employed to assess the effectiveness of potential decomposition candidates. While previous research has extensively addressed weight determination for control networks using the control affine state space model (Jogwar [2019], Tang and Daoutidis [2018]), our study introduces a generalized graph weighting methodology applicable to a broader spectrum of state space models, catering to both estimation and control purposes. In constructing the dynamic adjacency matrix, we represent the magnitude of the input-state, state-state, and state-output impacts by $\left|\frac{\partial f_j}{\partial u_i}\right|$, $\left|\frac{\partial f_j}{\partial x_i}\right|$, and $\left|\frac{\partial g_j}{\partial x_i}\right|$, respectively. The diagram presented in Figure 3 illustrates an es-

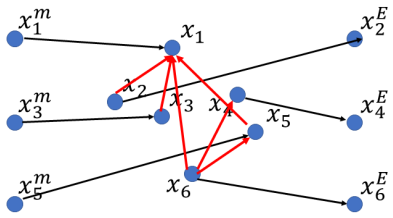

Fig. 3. Estimation network

timation network. In this network configuration, the measured states function as inputs, while the immeasurable states serve as outputs. For clarity, the nodes designated as "measured" and "unmeasured" have been intentionally included in the diagram.

This work endeavors to refine the spectral community detection framework (Newman [2013], Zhang and Newman [2015]), particularly in light of creating a weighted adjacency matrix. To identify the most optimal decomposition, a precise representation of modularity is considered as follows,

$$Q = \frac{1}{m}\sum_{ij}\left[A_{ij} - \frac{d_i d_j}{m}\right]\delta_{g_i,g_j} \tag{12}$$

where d_i denotes the sum of weights from all edges directed towards node i, and d_j represents the sum of weights from all edges emanating from node j. The total weight of all edges in the graph is denoted by m. The Kronecker delta is symbolized by δ. Eq. 12 computes the ratio of the total edge weight covered by communities to its expected value. In this equation, A_{ij} represents the weight of the edge connecting vertices j and i, while $\frac{d_i d_j}{m}$ signifies the expected value in a randomized graph. The term δ_{g_i,g_j} restricts the summation to pairs belonging to the same communities. By introducing the modularity matrix as $B_{ij} = A_{ij} - \frac{d_i \cdot d_j}{m}$ and its symmetrical counterpart $B_1 = B + B^T$, the modularity can be expressed as follows,

$$Q = \frac{1}{m}\sum_{ij} B_{1,ij}\delta_{g_i,g_j} \tag{13}$$

Utilizing the spectral community detection approach necessitates assigning two distinct types of vectors: one allocated to each node and another designated for each subsystem.

3.1 Node vector assignment

Employing eigen decomposition, B_1 can be represented as

$$B_{1,ij} = \sum_{l=1}^{N}\lambda_l U_{il} U_{jl} \tag{14}$$

where λ_l denotes the eigenvalue of B_1 corresponding to the l^{th} position, and U_{il} is the element associated with the orthogonal eigenvector matrix U. Additionally, the Kronecker delta can be alternatively expressed as

$$\delta_{g_i,g_j} = \sum_{s=1}^{P}\delta_{s,g_i}\delta_{s,g_j}. \tag{15}$$

By incorporating Eqs. 15 and 14 into the modularity equation (Eq. 13), the modularity can be modified as follows,

$$\begin{aligned} Q &= \frac{1}{m}\sum_{ij=1}^{N}\sum_{l=1}^{N}\lambda_l U_{il}U_{jl}\sum_{s=1}\delta_{s,gi}\delta_{s,gj} \\ &= \frac{1}{m}\sum_{l=1}^{N}\lambda_l\sum_{s=1}^{P}\left(\sum_{i=1}^{N}U_{il}\delta_{s,gi}\right)^2 \end{aligned} \tag{16}$$

The spectral community detection approach is based on Eq. 16, wherein a vector is assigned to each node. This equation implies that maximal modularity is attained by considering all positive eigenvalues in the node's vector definition. Nevertheless, this method renders the community detection process time-consuming and inefficient. To mitigate this challenge, we introduce the subsequent energy function,

$$E = \frac{\sum_{i=1}^{O}\lambda_{N-i}}{\sum_{i=1}^{N}\lambda_{N-i+1}} > \epsilon \tag{17}$$

where ϵ denotes the threshold for the count of positive eigenvalues. This threshold selectively retains only the dominant eigenvalues in the node's vector definition during the community detection. This strategic application of ϵ accelerates the community detection process while preserving accuracy within a predefined acceptable range of ϵ,

$$Q = \frac{1}{m}\sum_{l=1}^{O}\sum_{s=1}^{P}\left(\sum_{i=1}^{N}\sqrt{\lambda_l}U_{il}\delta_{s,gi}\right)^2 \tag{18}$$

Given this, a vector for each node, denoted as $[r_i]_l$, can be expressed as $[r_i]_l = \sqrt{\lambda_l}U_{il}$. Eq. 18 can then be condensed to

$$Q = \frac{1}{m}\sum_{s=1}^{P}\sum_{l=1}^{O}\left(\sum_{i}[r_i]_l\right)^2 = \frac{1}{m}\sum_{s=1}^{P}\left|\sum_{i} r_i\right|^2 \tag{19}$$

By introducing the notation $R_s = \sum_i r_i$, the modularity can be expressed as

$$Q = \frac{1}{m}\sum_{s}|R_s|^2 \tag{20}$$

3.2 Community detection algorithm

Eq. 20 defines modularity in terms of subsystem vectors. This formulation identifies the optimal subsystem for vertex i within the range of options from A to B. The alteration in modularity value is computed by assessing the transition of node i from B to A."(21) The optimal sub-community for node i is determined by maximizing the positive change in modularity. As delineated in Zhang and Newman [2015], spectral community detection employs a recursive approach involving representative vectors, inner product computations, and node assignments to optimize modularity. Initially, representative vectors are established based on an initial guess, ensuring that the sum of all elements in vector $\mathbf{R}_i$ is zero. Subsequently, the inner product of each representative vector with the vector representing all vertices is calculated, identifying the group to which the node is closest. Vertices are then assigned to the representative vector with the highest inner product value. The representation is refined by aggregating all vectors within each subsystem, generating new vectors $\mathbf{R}$ for each community. This iterative process continues until no further modifications occur.

4. CHEMICAL PROCESS NETWORK CASE STUDY

Spectral community detection was employed with a weighted graph representation of a benchmark integrated benzene alkylation process (Fig. 4) to identify an optimal architecture for distributed control and estimation. The performance of the determined communities was systematically evaluated under diverse operational conditions, focusing on analyzing the closed-loop performance at varying reflux ratios, specifically medium and low values. The

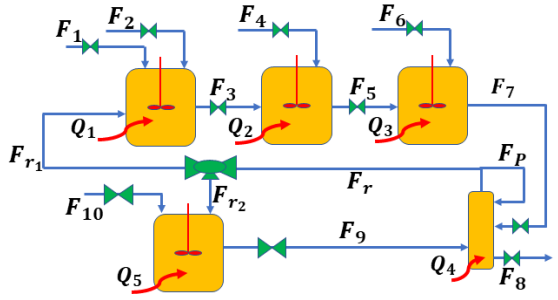

Fig. 4. Benzene alkylation process.

benzene alkylation process with ethylene involves four key components: benzene (A), ethylene (B), ethylbenzene (C), and 1,3-diethylbenzene (D). The following chemical reactions take place within the first three continuous stirred tank reactors (CSTRs),

Reaction #1: A + B → C
Reaction #2: C + B → D

and the following reaction occurs in the fourth CSTR,

Reaction #3: A + D → C

The benzene alkylation process produces ethylbenzene (C) as the desired product, with the unintended byproduct of 1,3-diethylbenzene (D). Pure benzene is fed to the first CSTR, and the other CSTRs are supplied with pure ethylene. The resulting effluent stream, comprising benzene (A), ethylene (B), ethylbenzene (C), and 1,3-diethylbenzene (D), is directed to the separator. From the bottom fraction of the separator, ethylbenzene (C) is extracted, where most benzene is separated and recycled for use in the first and fourth CSTRs. Additionally, 1,3-diethylbenzene (D) is introduced into the final CSTR to facilitate the synthesis of ethylbenzene. The mathematical model of the process (Liu et al. [2010], Pourkargar et al. [2019]) involves a set of 30 ordinary differential equations (ODEs) describing the holdup (V), temperature (T), and key component concentrations (C_A, C_B, C_C, and C_D) within the four CSTRs (process units 1, 2, 3, and 5) and the separator (process unit 4). The control objective is to regulate the holdup, temperature, and ethylbenzene concentrations in the CSTRs and the separator by adjusting the 12 flow rates and 5 heat flow rates supplied to the process units.

4.1 Distributed estimation and control

This case study investigated the system under two defined operating scenarios: medium recycle, characterized by a recycle ratio of $R = 1$, and low recycle, featuring a recycle ratio of $R = 0.001$. The system decompositions were obtained employing the proposed spectral community detection method, utilizing the energy function and the weighted adjacency matrix of estimation and control for both operating scenarios. Furthermore, using an unweighted adjacency matrix that remains constant for $R = 1$ and $R = 0.001$, facilitated an unweighted decomposition, aligning with the results presented in Pourkargar et al. [2019]. Tables 1 and 2 summarize the distribution of the variables among the control and estimation agents assigned to the subsystems, accompanied by the corresponding modularity values. The decomposition analysis

Table 1. Distributed control structures.

Control agents	Weighted (R=0.001)	Weighted (R=1)	Unweighted
C_1	F_1 F_3 F_5 F_7 F_{R_2} V_3 T_1 C_{C_1} C_{C_2} C_{C_3}	F_1 F_3 F_5 F_7 F_{R_2} C_{C_1} C_{C_2} T_1 C_{C_3}	F_1 F_2 F_3 F_4 F_{R_2} Q_1 V_1 V_2 C_{C_2} T_1 T_2 C_{C_1}
C_2	F_2 F_4 V_2 T_2	F_4 F_6 F_{10} V_2 T_2 T_3	F_5 F_6 F_7 Q_3 V_3 T_3 C_{C_3}
C_3	F_6 F_8 F_9 F_{10} F_{R1} Q_1 Q_2 Q_3 Q_4 Q_5 V_4 V_5 T_3 T_4 T_5 V_1 C_{C_4} C_{C_5}	F_2 F_8 F_9 F_{R_1} Q_1 Q_2 Q_3 Q_4 Q_5 V_3 V_4 V_5 T_4 T_5 C_{C_4} C_{C_4} V_1	F_8 F_9 F_{10} F_{R_1} Q_4 Q_5 T_4 V_4 V_5 T_4 T_5 C_{C_4} C_{C_5}
Q	0.6025	0.6017	0.2953

results, encompassing both estimation and control aspects, underscore a notable distinction between the decomposition patterns of the weighted adjacency matrix under different operating conditions and those of the unweighted adjacency matrix. Furthermore, the findings illustrate that the most favorable decomposition varies across operating conditions, particularly at $R = 1$ and $R = 0.001$.

4.2 Simulation results and discussions

An integrated DMHE and DMPC structure was designed based on the spectral community detection of the weighted and unweighted graph representations of the benzene alkylation process. The closed-loop performance for the output

Table 2. Distributed estimation structures.

Estimation agents	Weighted (R=1)	Weighted (R=0.001)	Unweighted
E_1	$V_1\ V_4\ T_1\ T_4\ C_{A_1}\ C_{B_1}\ C_{C_1}\ C_{D_1}$	$V_1\ T_1\ C_{A_1}\ C_{B_1}\ C_{C_1}\ C_{D_1}$	$V_1\ T_1\ C_{A_1}\ C_{B_1}\ C_{C_1}\ C_{D_1}$
E_2	$V_2\ T_2\ C_{A_2}\ C_{B_2}\ C_{C_2}\ C_{D_2}$	$V_2\ T_2\ C_{A_2}\ C_{B_2}\ C_{C_2}\ C_{D_2}$	$V_2\ T_2\ C_{A_2}\ C_{B_2}\ C_{C_2}\ C_{D_2}$
E_3	$V_3\ T_3\ C_{A_3}\ C_{B_3}\ C_{C_3}\ C_{D_3}\ C_{A_4}\ C_{B_4}\ C_{C_4}\ C_{D_4}$	$V_3\ T_3\ V_4\ C_{A_3}\ C_{B_3}\ C_{C_3}\ C_{D_3}\ C_{A_4}\ C_{B_4}\ C_{C_4}$	$V_3\ T_3\ C_{A_3}\ C_{B_3}\ C_{C_3}\ C_{D_3}$
E_4	$V_5\ T_5\ C_{A_5}\ C_{B_5}\ C_{C_5}\ C_{D_5}$	$V_5\ T_4\ T_5\ C_{D_4}\ C_{A_5}\ C_{B_5}\ C_{C_5}\ C_{D_5}$	$V_4\ V_5\ T_4\ T_5\ C_{A_4}\ C_{B_4}\ C_{D_4}\ C_{A_5}\ C_{B_5}\ C_{C_5}\ C_{D_5}$
Q	0.7332	0.7342	0.5467

regulation problem is evaluated for both weighted and unweighted decompositions, detailed in Section 4.1. The number of control and estimation agents corresponds to the number of subsystems, as indicated in Tables 1 and 2. We set control and estimation horizons of 10 minutes and a sampling interval of 1 minute. Within the estimation framework, white noise with a signal-to-noise ratio of 20 to the process model is considered to interfere with measured outputs. The weighting matrices for estimation and control were chosen to balance the importance of output regulation errors, manipulated inputs, and observed noise within the objective functions. Upper and lower boundaries for manipulated inputs and estimated states were set at ±%20 of the reference steady state values. The underlying dynamic optimization for estimation and control problems was solved at each sampling time by the interior point optimization (IPOPT) method (Biegler [2010]). The performance of the closed-loop system was consistently observed by monitoring holdups, temperatures, and ethylbenzene concentrations.

Figures 5 and 6 illustrate the temporal profiles of two selected controlled outputs (CSTR temperature and ethylbenzene concentration) and two selected manipulated inputs (feed flow rate and heat flow) for $R = 1$ and $R = 0.001$. The figures illustrate a more gradual convergence

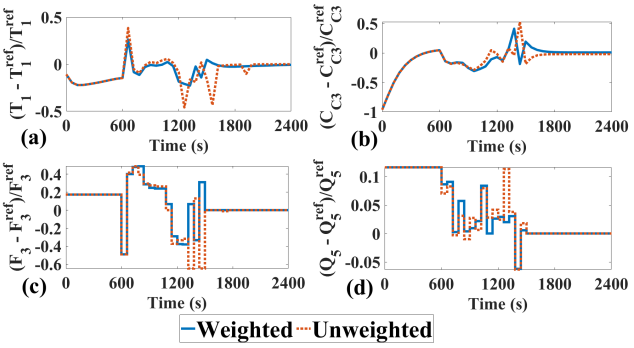

Fig. 5. Temporal profiles of selected state variables and manipulated inputs under integrated DMHE and DMPC based on the decomposition obtained from weighted graph representation for $R = 1$ and unweighted graph representation: (a) first CSTR temperature, (b) ethylbenzene concentration leaving the third CSTR, (c) flow rate from the first CSTR to the second CSTR, and (d) heat provided to the fourth CSTR.

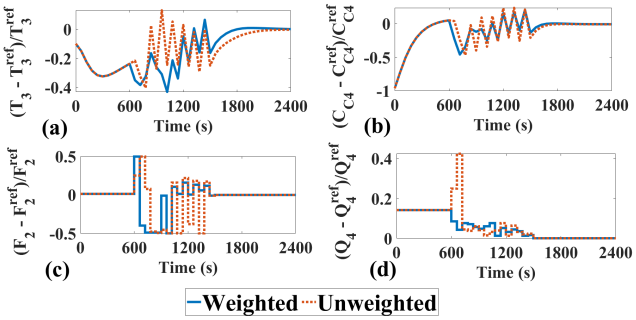

Fig. 6. Temporal profiles of selected state variables and manipulated inputs under integrated DMHE and DMPC based on the decomposition obtained from weighted graph representation for $R = 0.001$ and unweighted graph representation: (a) third CSTR temperature, (b) ethylbenzene concentration leaving the separator, (c) ethylene feed flow rate to the first CSTR, and (d) heat provided to the separator.

to the desired value when utilizing weighted decomposition. Furthermore, the variation in control action is less erratic when employing weighted decomposition than unweighted decomposition. The dimensionless performance index (DPI), introduced in Pourkargar et al. [2019], is a performance metric with lower values showing lower output regulation error and manipulated inputs. The performance comparison is summarized in Figs. 7 and 8 for medium and low recycle ratios.

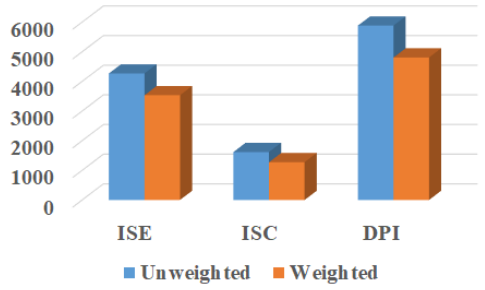

Fig. 7. Closed-loop performance for $R = 1$.

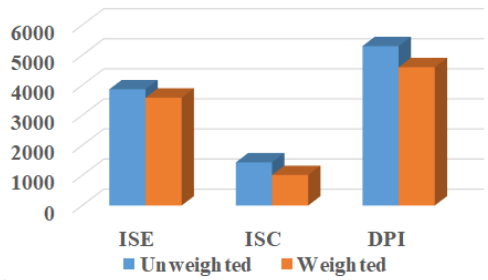

Fig. 8. Closed-loop performance for $R = 0.001$.

The integrated DMHE and DMPC structure at the medium recycle ratio shows a %18.3 improvement in DPI when using a weighted graph decomposition. This improvement reduces to %13.2 for low recycling. The observed enhancement can be attributed to the strategic utilization of a weighted network, wherein each agent makes decisions more optimally, closely resembling a scenario in which control and estimation agents operate autonomously.

5. CONCLUSION

An adaptive spectral community detection-based decomposition approach was developed for distributed state estimation and control of highly integrated process systems. A weighted graph representation of the system was used to identify the optimal decompositions under different operational conditions. An integrated DMHE and DMPC structure has been synthesized based on the proposed system decomposition strategy to address the output regulation problem of integrated processes. A benchmark benzene alkylation process was used to illustrate the effectiveness of the distributed estimation and control approach. The closed-loop simulation results were analyzed for decompositions based on both weighted and unweighted graph representations of the benzene alkylation process. The findings highlighted a substantial enhancement in the overall efficiency of the closed-loop performance when adopting the weighted graph representation and adaptive community detection approaches. This is attributed to the exceptional capacity of the proposed approach to capture not just the presence of interactions but also to quantify the intensity of interactions among various components of the process network.

REFERENCES

Baldea, M. and Daoutidis, P. (2012). *Dynamics and nonlinear control of integrated process systems*. Cambridge University Press.

Biegler, L.T. (2010). *Nonlinear programming: concepts, algorithms, and applications to chemical processes*. SIAM.

Copp, D.A. and Hespanha, J.P. (2014). Nonlinear output-feedback model predictive control with moving horizon estimation. In *53rd IEEE conference on decision and control*, 3511–3517. IEEE.

Copp, D.A. and Hespanha, J.P. (2017). Simultaneous nonlinear model predictive control and state estimation. *Automatica*, 77, 143–154.

Guay, M., Adetola, V., and DeHaan, D. (2015). *Robust and adaptive model predictive control of nonlinear systems*. Institution of Engineering and Technology.

Heo, S. and Daoutidis, P. (2016). Control-relevant decomposition of process networks via optimization-based hierarchical clustering. *AIChE Journal*, 62(9), 3177–3188.

Heo, S., Marvin, W.A., and Daoutidis, P. (2015). Automated synthesis of control configurations for process networks based on structural coupling. *Chemical Engineering Science*, 136, 76–87.

Jogwar, S.S. (2019). Distributed control architecture synthesis for integrated process networks through maximization of strength of input–output impact. *Journal of Process Control*, 83, 77–87.

Leicht, E.A. and Newman, M.E. (2008). Community structure in directed networks. *Physical review letters*, 100(11), 118703.

Liu, J., Chen, X., Muñoz de la Peña, D., and Christofides, P.D. (2010). Sequential and iterative architectures for distributed model predictive control of nonlinear process systems. *AIChE Journal*, 56(8), 2137–2149.

Lopez-Negrete, R., D'Amato, F.J., Biegler, L.T., and Kumar, A. (2013). Fast nonlinear model predictive control: Formulation and industrial process applications. *Computers & Chemical Engineering*, 51, 55–64.

Newman, M.E. (2006). Modularity and community structure in networks. *Proceedings of the national academy of sciences*, 103(23), 8577–8582.

Newman, M.E. (2013). Spectral methods for community detection and graph partitioning. *Physical Review E*, 88(4), 042822.

Pannocchia, G., Rawlings, J.B., and Wright, S.J. (2007). Fast, large-scale model predictive control by partial enumeration. *Automatica*, 43(5), 852–860.

Pourkargar, D.B., Almansoori, A., and Daoutidis, P. (2017a). Distributed model predictive control of process networks: Impact of control architecture. *IFAC-PapersOnLine*, 50(1), 12452–12457.

Pourkargar, D.B., Almansoori, A., and Daoutidis, P. (2017b). Impact of decomposition on distributed model predictive control: A process network case study. *Industrial & Engineering Chemistry Research*, 56(34), 9606–9616.

Pourkargar, D.B., Moharir, M., Almansoori, A., and Daoutidis, P. (2019). Distributed estimation and nonlinear model predictive control using community detection. *Industrial & Engineering Chemistry Research*, 58(30), 13495–13507.

Rao, C.V., Rawlings, J.B., and Mayne, D.Q. (2003). Constrained state estimation for nonlinear discrete-time systems: Stability and moving horizon approximations. *IEEE transactions on automatic control*, 48(2), 246–258.

Rawlings, J.B. and Bakshi, B.R. (2006). Particle filtering and moving horizon estimation. *Computers & Chemical Engineering*, 30(10-12), 1529–1541.

Rawlings, J.B., Mayne, D.Q., and Diehl, M. (2017). *Model predictive control: Theory, computation, and design*, volume 2. Nob Hill Publishing Madison, WI.

Schwenzer, M., Ay, M., Bergs, T., and Abel, D. (2021). Review on model predictive control: An engineering perspective. *The International Journal of Advanced Manufacturing Technology*, 117(5-6), 1327–1349.

Tang, W., Allman, A., Pourkargar, D.B., and Daoutidis, P. (2018a). Optimal decomposition for distributed optimization in nonlinear model predictive control through community detection. *Computers & Chemical Engineering*, 111, 43–54.

Tang, W. and Daoutidis, P. (2018). Network decomposition for distributed control through community detection in input–output bipartite graphs. *Journal of Process Control*, 64, 7–14.

Tang, W., Pourkargar, D.B., and Daoutidis, P. (2018b). Relative time-averaged gain array (RTAGA) for distributed control-oriented network decomposition. *AIChE Journal*, 64(5), 1682–1690.

Wang, Y. and Boyd, S. (2009). Fast model predictive control using online optimization. *IEEE Transactions on control systems technology*, 18(2), 267–278.

Yin, X., Decardi-Nelson, B., and Liu, J. (2018). Subsystem decomposition and distributed moving horizon estimation of wastewater treatment plants. *Chemical Engineering Research and Design*, 134, 405–419.

Yin, X. and Liu, J. (2019). Subsystem decomposition of process networks for simultaneous distributed state estimation and control. *AIChE Journal*, 65(3), 904–914.

Zhang, X. and Newman, M.E. (2015). Multiway spectral community detection in networks. *Physical Review E*, 92(5), 052808.